Inorg. Chem. **2008**, *47*, 2477−2484

Hydrogen Storage in Mesoporous Titanium Oxide−Alkali Fulleride Composites

Xin Hu,[†] **Michel Trudeau**,[‡] **and David M. Antonelli***,[†]

Department of Chemistry and Biochemistry, University of Windsor, Windsor, Ontario N9B 3P4, Canada, and Chemistry and Materials, Hydro-Québec Research Institute, Varennes, Quebec J3X 1S1, Canada

Received September 7, 2007

Mesoporous titanium oxide−alkali fulleride composites were synthesized and characterized by X-ray diffraction, nitrogen adsorption, Raman spectroscopy, and elemental analysis. The hydrogen sorption properties of these composites were investigated at 77 K, room temperature, and 200 °C. A maximum overall volumetric uptake of 27.35 kg/m^3 was obtained for the lithium fulleride composite at 77 K and 100 atm, compared with 25.48 kg/m^3 for the pristine unreduced material under the same conditions. This value was less than those previously reported for bis(toluene)titanium- and bis(benzene)vanadium-reduced materials (40.46 and 33.42 kg/m^3, respectively) and also less than those found for the fulleride-free Li- and Na-reduced materials in this study (28.10 and 28.19 kg/m^3, respectively). At room temperature and 100 atm, the maximum gravimetric storage and adsorption values of fulleride-impregnated composites were 0.99 and 0.11 wt %, respectively, while the corresponding amounts for unreduced material were 0.94 and 0.10 wt %. At 200 °C and 100 atm, the maximum gravimetric storage and adsorption capacities of fulleride composites were less than those of the unreduced material, which were 0.62 and 0.06 wt %, respectively. Thus, inclusion of fulleride units in the pores lowered the overall gravimetric and volumetric storage relative to the fulleride-free Na- and Li-reduced counterparts. Like other reduced composites studied in our group, the enthalpies of the reduced composites showed an unusual increasing trend with surface coverage, with the greatest value (6.55 kJ/mol) measured for the Na-reduced fulleride composite. This suggests that the reduced titanium oxide surface provides the majority of the binding sites in these materials.

Introduction

Hydrogen storage has recently attracted much interest because hydrogen is an ideal energy carrier[1] and has the potential to replace customary fossil fuels (i.e., petroleum, coal, and natural gas), which are not only limited in supply but also harmful to the environment. Compressed hydrogen gas and cryogenically stored (20 K) liquid hydrogen are the simplest technologies for hydrogen storage; however, the former suffers from low storage density as well as safety concerns due to the high pressures required, while the large amount of energy required for liquefaction and boil-off of liquid hydrogen are significant drawbacks for the latter. To overcome these problems, solids which absorb hydrogen reversibly with high gravimetric and volumetric densities at moderate temperatures and pressures are being sought. Metal alloys[2] and metal hydrides[3] have been studied at temperatures over 100 °C.[4] However, even the best of these materials displays unfavorable kinetics, poor reusability, and low thermal conductivity. As an alternative to metal hydrides, a wide variety of porous materials, including carbon-based nanostructured materials,[5–14] zeolites,[15–20] and microporous

* To whom correspondence should be addressed. E-mail: danton@uwindsor.ca.
[†] University of Windsor.
[‡] Hydro-Québec Research Institute.

(1) Schlapbach, L.; Züttel, A. *Nature* **2001**, *414*, 353.
(2) Yartys, V. A.; Harris, I. R.; Panasyuk, V. V. *Mater. Sci.* **2001**, *37*, 219.
(3) Sandrock, G. A. *J. Alloys Compd.* **1999**, *877*, 293.
(4) Seayad, A. M.; Antonelli, D. M. *Adv. Mater.* **2004**, *16*, 765.
(5) Dillon, A. C.; Jones, K. M.; Bekkedahl, T. A.; Kiang, C. H.; Bethune, D. S.; Heben, M. J. *Nature* **1997**, *386*, 377.
(6) Chen, P.; Wu, X.; Lin, J.; Tan, K. L. *Science* **1999**, *285*, 91.
(7) Ye, Y.; Ahn, C. C.; Witham, C.; Fultz, B.; Liu, J.; Rinzler, A. G.; Colbert, D.; Smith, K. A.; Smalley, R. E. *Appl. Phys. Lett.* **1999**, *74*, 2307.
(8) Liu, C.; Fan, Y. Y.; Liu, M.; Cong, H. T.; Cheng, H. M.; Dresselhaus, M. S. *Science* **1999**, *286*, 1127.

10.1021/ic701762e CCC: $40.75
Published on Web 02/23/2008

metal−organic frameworks (MOFs),[21–36] have been studied at liquid-nitrogen temperature. Since these materials have exceptionally high specific surface areas combined with beneficial microporosities and relatively low skeletal densities, many of them have shown promising gravimetric hydrogen uptake at 77 K via physisorption of hydrogen to the porous framework.[7,26] However, to date there has been no report of any material meeting or surpassing the 2015 U.S. Department of Energy (DOE) target values (9 wt % and 81 kg/m^3 for gravimetric and volumetric hydrogen storage, respectively).

Recent advances within our group have demonstrated that micro- and mesoporous titanium oxides could serve as hosts for hydrogen storage.[4] (According to IUPAC definitions, inorganic solids with pore sizes of <20 and 20−500 Å are considered to be microporous and mesoporous materials, respectively.) Micro- and mesoporous titanium oxides contain ordered arrays of channels that allow hydrogen to effectively access their interior spaces. The pore size, surface area, and wall thickness can be systemically modified to improve hydrogen uptake.[37] A unique property of these materials is their ability to act as electron acceptors as a result of their capacity to have variable oxidation states in the transition-metal oxide walls of the micro- and mesoporous structure,[38] a feature not present in MOFs, zeolites, or porous carbon. This exceptional property combined with the coordinative unsaturation of Ti centers is likely to improve hydrogen storage capacities because binding of H_2 to transition metals is strongly dependent on the electron density at the metal center and its ability to back-bond through a π interaction into the H−H antibonding orbital.[39–41]

The hypothesis that low-valence metal surfaces can bind hydrogen more effectively was verified by work in our group that showed that chemically reduced microporous titanium oxides are more effective hydrogen storage materials than the parent unreduced material.[42,43] For example, microporous titanium oxide treated with bis(toluene)titanium demonstrated a reversible gravimetric storage capacity of 4.94 wt % with a volumetric storage capacity of more than 40 kg/m^3 at 77 K and 100 atm, and microporous titanium oxide reduced with Na (Li) showed reversible gravimetric and volumetric storage capacities of 5.58 (5.63) wt % and 31.58 (31.30) kg/m^3, respectively.[42] These values were all significantly larger than those for the unreduced titanium oxide material, whose reversible gravimetric and volumetric densities were 5.36 wt % and 29.37 kg/m^3, respectively.[42] For all of these reduced materials, reduction of the surface led to a dramatic change in surface properties, resulting in higher enthalpies of adsorption as well as the first example of enthalpies that increased upon hydrogen loading, suggesting a different mechanism than simple physisorption.

Preliminary work conducted by our group in collaboration with General Motors (GM)[4] suggested that mesoporous titanium oxides reduced with alkali fullerides may possess a maximum gravimetric uptake of 9 wt % at 200 °C and 100 atm. This family of composites is related to mesoporous tantalum or niobium oxide−alkali fulleride intercalates previously studied by our group.[44–50] These materials possess reduced transition-metal oxide walls with one-dimensional (1D) chains of alkali fullerides filling the porous channels. They can also be readily tuned by addition of more alkali metal reductant, sometimes resulting in dramatically different

(9) Poirier, E.; Chahine, R.; Benard, P.; Cossement, D.; Lafi, L.; Melancon, E.; Bose, T. K.; Deilets, S. *Appl. Phys. A: Mater. Sci. Process.* **2004**, *78*, 961.
(10) Tibbetts, G. G.; Meisner, G. P.; Olk, C. H. *Carbon* **2001**, *39*, 2291.
(11) Nijkamp, M. G.; Raaymakers, J. E. M. J.; van Dillen, A. J.; de Jong, K. P. *Appl. Phys. A: Mater. Sci. Process.* **2001**, *72*, 619.
(12) Schimmel, H. G.; Kearley, G. J.; Nijkamp, M. G.; Visser, C. T.; de Jong, K. P.; Mulder, F. M. *Chem.−Eur. J.* **2003**, *9*, 4764.
(13) Benard, P.; Chahine, R. *Langmuir* **2001**, *17*, 1950.
(14) Zuttel, A.; Sudan, P.; Mauron, P.; Emmenegger, S.; Schlapbach, L. *Int. J. Hydrogen Energy* **2002**, *27*, 203.
(15) Zecchina, A.; Bordiga, S.; Vitillo, J. G.; Ricchiardi, G.; Lamberti, C.; Spoto, G.; Bjorgen, M.; Lillerud, K. P. *J. Am. Chem. Soc.* **2005**, *127*, 6361.
(16) Arean, C. O.; Delgado, M. R.; Palomino, G. T.; Rubio, M. T.; Tsyganenko, N. M.; Tsyganenko, A. A.; Garrone, E. *Microporous Mesoporous Mater.* **2005**, *80*, 247.
(17) Langmi, H. W.; Walton, A.; Al-Mamouri, M. M.; Johnson, S. R.; Book, D.; Speight, J. D.; Edwards, P. P.; Gameson, I.; Anderson, P. A.; Harris, I. R. *J. Alloys Compd.* **2003**, *710*, 356.
(18) Kazansky, V. B.; Borovkov, V. Y.; Serich, A.; Karge, H. G. *Microporous Mesoporous Mater.* **1998**, *22*, 251.
(19) Vitillo, J. G.; Ricchiardi, G.; Spoto, G.; Zecchina, A. *Phys. Chem. Chem. Phys.* **2005**, *7*, 3948.
(20) Langmi, H. W.; Book, D.; Walton, A.; Johnson, S. R.; Al-Mamouri, M. M.; Speight, J. D.; Edwards, P. P.; Harris, I. R.; Anderson, P. A. *J. Alloys Compd.* **2005**, *637*, 404.
(21) Rosi, N. L.; Eckert, J.; Eddoudi, M.; Vodak, D. T.; Kim, J.; O'Keeffe, M.; Yaghi, O. M. *Science* **2003**, *300*, 1127.
(22) Rowsell, J. L. C.; Milward, A. R.; Park, K. S.; Yaghi, O. M. *J. Am. Chem. Soc.* **2004**, *126*, 5666.
(23) Rowsell, J. L. C.; Yaghi, O. M. *Angew. Chem., Int. Ed.* **2005**, *44*, 4670.
(24) Panella, B.; Hirscher, M. *Adv. Mater.* **2005**, *17*, 538.
(25) Kaye, S. S.; Long, J. R. *J. Am. Chem. Soc.* **2005**, *127*, 6506.
(26) Wong-Foy, A. G.; Matzger, A. J.; Yaghi, O. M. *J. Am. Chem. Soc.* **2006**, *128*, 3494.
(27) Zhao, X.; Xiao, B.; Fletcher, A. J.; Thomas, K. M.; Bradshaw, D.; Rosseinsky, M. J. *Science* **2004**, *306*, 1012.
(28) Dybstev, D. N.; Chun, H.; Yoon, S. H.; Kim, D.; Kim, K. *J. Am. Chem. Soc.* **2004**, *126*, 32.
(29) Ferey, G.; Latroche, M.; Serre, C.; Millange, F.; Loiseau, T.; Percheron-Guegan, A. *Chem. Commun.* **2003**, 2976.
(30) Dybstev, D. N.; Chun, H.; Kim, K. *Angew. Chem., Int. Ed.* **2004**, *43*, 5033.
(31) Pan, L.; Sander, M. B.; Huang, X.; Li, J.; Smith, M.; Bittner, E.; Bockrath, B.; Johnson, J. K. *J. Am. Chem. Soc.* **2004**, *126*, 1308.
(32) Kubota, Y.; Takata, M.; Matsuda, R.; Kitaura, R.; Kitagawa, S.; Kato, K.; Sakata, M.; Kobayashi, T. C. *Angew. Chem., Int. Ed.* **2005**, *44*, 920.
(33) Dinca, M.; Yu, A.; Long, J. *J. Am. Chem. Soc.* **2006**, *128*, 8904.
(34) Peterson, V.; Liu, Y.; Brown, C.; Kepert, C. *J. Am. Chem. Soc.* **2006**, *128*, 15578.
(35) Foster, P.; Eckert, J.; Heiken, B.; Parise, J.; Yoon, J.; Jhung, S.; Chang, J.; Cheetham, A. *J. Am. Chem. Soc.* **2006**, *128*, 16846.
(36) Dinca, M.; Dailly, A.; Liu, Y.; Brown, C.; Neumann, D.; Long, J. *J. Am. Chem. Soc.* **2006**, *128*, 16876.
(37) Antonelli, D. M. *Microporous Mesopororous Mater.* **1999**, *30*, 315.
(38) He, X.; Antonelli, D. M. *Angew. Chem., Int. Ed.* **2002**, *41*, 214.
(39) Kubas, G. J. *J. Organomet. Chem.* **2001**, *635*, 37.
(40) Zhao, Y.; Kim, Y.-H.; Dillon, A. C.; Heben, M. J.; Zhang, S. B. *Phys. Rev. Lett.* **2005**, *94*, 155504.
(41) Yildirim, T.; Ciraci, S. *Phys. Rev. Lett.* **2005**, *94*, 175501.
(42) Hu, X.; Skadtchenko, B. O.; Trudeau, M.; Antonelli, D. M. *J. Am. Chem. Soc.* **2006**, *128*, 11740.
(43) Hu, X.; Trudeau, M.; Antonelli, D. M. *Chem. Mater.* **2007**, *19*, 1388.
(44) Ye, B.; Trudeau, M.; Antonelli, D. M. *Adv. Mater.* **2001**, *13*, 29.
(45) Ye, B.; Trudeau, M.; Antonelli, D. M. *Adv. Mater.* **2001**, *13*, 561.
(46) Ye, B.; Trudeau, M.; Antonelli, D. M. *Chem. Mater.* **2001**, *13*, 2730.
(47) Ye, B.; Trudeau, M.; Antonelli, D. M. *Chem. Mater.* **2002**, *14*, 2774.
(48) Skadtchenko, B. O.; Trudeau, M.; Schurko, R. W.; Willans, M. J.; Antonelli, D. *Adv. Funct. Mater.* **2003**, *13*, 671.
(49) Skadtchenko, B. O.; Trudeau, M.; Kwon, C. W.; Dunn, B.; Antonelli, D. *Chem. Mater.* **2004**, *16*, 2886.
(50) Skadtchenko, B. O.; Trudeau, M.; Schurko, R. W.; Lo, A. Y. H.; Antonelli, D. M. *Chem. Mater.* **2005**, *17*, 1467.

conductivity properties. Although these preliminary results at 200 °C proved to be unreliable, we reasoned that the reduced fulleride units may act as additional sites for cryogenic hydrogen binding in a mesoporous Ti oxide framework while also creating microporous cavities within the mesoporous gallery, possibly enhancing absorption of hydrogen through capillary effects. The pseudographitic nature of the C_{60} surface is directly analogous to that of the walls of many carbon-based hydrogen storage materials and could thus provide additional carbon-based hydrogen binding sites within the mesoporous channels, which would otherwise be filled with compressed gas. In order to more fully explore the hydrogen storage properties of these new composites, we synthesized a series of sodium and lithium fulleride-impregnated mesoporous titanium oxide composites and screened them at a variety of temperatures and pressures.

Experimental Section

Materials and Equipment. All chemicals were obtained from Aldrich, unless stated otherwise. Trimethylsilyl chloride was obtained from Alfa and distilled over calcium hydride. Mesoporous titanium oxide samples were dried at 150 °C overnight under vacuum and then stirred with excess trimethylsilyl chloride in dry ether for 12 h under nitrogen. This capped internal OH groups that could interfere with redox reactions and lead to degradation of the mesostructure. Nitrogen adsorption/desorption data were collected on a Micromeritics ASAP 2010 analyzer. X-ray diffraction (XRD) patterns were recorded in a sealed glass capillary using a Siemens D-500 $\theta-2\theta$ diffractometer with Cu Kα radiation. Raman spectra were recorded using a Renishaw Ramascope equipped with a Renishaw 514 nm Diode Laser System. The skeletal densities of the samples were measured using a Quantachrome Micro-Ultrapycnometer 1000 with helium gas. Determination of the apparent density of the material is a common practice and is readily accomplished by dividing the mass of the packed powder by the volume it occupies. All of the elemental analysis data (conducted under an inert atmosphere) were obtained from Galbraith Laboratories (Knoxville, TN).

H_2 Sorption Measurements. Hydrogen adsorption/desorption isotherms were measured using a commercial computer-controlled gas reaction controller (GRC) obtained from Advanced Materials Corp. (Pittsburgh, PA). Highly purified (99.9995%) hydrogen was used as the adsorbate. Typically, the mass required for the hydrogen sorption measurement was 500–1000 mg. The size of the sample chamber was 2.5 cm^3. Lightly packed powder materials were used for all measurements. Before each measurement, the materials were degassed at 200 °C under a vacuum of 10^{-3} Torr for at least 1 day in order to remove any physisorbed water or volatile impurities. A simplified sketch of this apparatus is shown below:

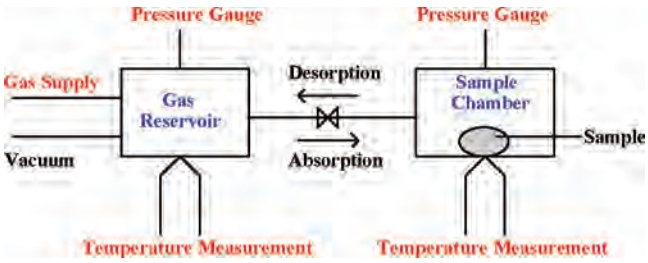

The temperature of the gas reservoir was measured with two AD590 IC thermometers calibrated within 0.1 °C against a standard mercury thermometer at room temperature. The sample temperature was measured with a K-type thermocouple by converting voltage readings to temperatures according to ITS-90 (the International Temperature Scale of 1990). Error limits were 2 °C (0.75%) and 2 °C (2%) above and below 0 °C, respectively. The pressures in the gas reservoir and sample chamber were measured using Heise model HP0 pressure transducers having a full-scale range of 1500 psi (100 atm). The accuracy of this transducer was rated to be 0.05% of the full-scale range, including nonlinearity, drift, and hysteresis.

The GRC operates as follows. An appropriate amount of gas is added to the gas reservoir, and the molar amount of this gas is determined from its pressure and temperature. The system then manipulates the valves between the reservoir and the sample chamber in order to transfer the desired amount of the gas from the former to the latter. After equilibrium is attained, the system recalculates the number of hydrogen molecules, and the number missing from the gas phase corresponds to the number of molecules adsorbed by the sample. The system employs a modified Benedict−Webb−Rubin equation of state in calculating the amount of adsorbed hydrogen from the pressure, temperature, and volume. The apparatus gradually increases the hydrogen pressure to the maximum specified value while summing the adsorbed hydrogen. The amount of hydrogen released from the sample is then determined by pumping out the gas reservoir and then gradually bleeding hydrogen from the sample chamber into the gas reservoir. During the test process, the sample chamber is immersed in liquid nitrogen, and the liquid level is maintained. This apparatus effectively measures the pressure of the hydrogen in the sample chamber and then calculates the number of moles on the basis of this pressure, the temperature, and the volume [corrected by subtracting the sample volume (obtained by direct input of the sample weight and density) from the empty chamber volume]. If the density used is the skeletal density measured by a pycnometer, the compressed hydrogen within the pores is treated as part of the sample chamber volume, but if the apparent density of the sample is used instead, the compressed gas in the pores is treated as having been adsorbed by the sample along with the hydrogen physisorbed to the walls of the skeletal structure. The advantage of this system is that it obviates the need for assumptions about the void space volume of the material in order to obtain the total amount of H_2 in the system (including the compressed gas in the void space), which is crucial in determining the amount of useful fuel stored in the material. Most other Sieverts apparatuses work by automatically subtracting out the compressed gas in the pores, thus eliminating the use of the pycnometer but making the determination of the amount of compressed gas in the pores more ambiguous. Gravimetric adsorption (equivalent to what is often called "excess storage") and total storage are measured directly, whereas the two volumetric density values are calculated using the apparent densities.

Enthalpies of adsorption were calculated from the hydrogen adsorption data at 77 and 87 K using a variant of the Clausius−Clapeyron equation:[51]

$$\ln\left(\frac{P_1}{P_2}\right) = \Delta H_{ads}\left(\frac{T_2 - T_1}{RT_1T_2}\right) \quad (1)$$

where P_n and T_n are the pressure and temperature for isotherm n, respectively, and R is the gas constant. Pressure as a function of the amount of gas adsorbed was determined using an exponential fit for each isotherm. This exponential equation gave an accurate fit for pressures up to 10 atm, with a goodness of fit (R^2) value

(51) Rouquerol, F.; Rouquerol, J.; Sing, K. *Adsorption by Powders and Porous Solids: Principles, Methodology and Applications*; Academic Press: London, 1999.

greater than 0.99. The P_n values corresponding to a particular amount of adsorbed H_2 at the isotherm temperatures T_n were obtained from the exponential fit equations for the two isotherms. Substituting these values into eq 1 yielded the enthalpy of adsorption.

Synthesis Procedures. Mesoporous Titanium Oxide Materials. In a typical preparation, titanium(IV) isoproxide (15 g, 52.77 mmol) was warmed with dodecylamine (4.89 g, 26.39 mmol) until a homogeneous, colorless solution was obtained. To this solution was added 75 mL of water with stirring. Precipitation occurred immediately. HCl (37%, 0.2603 g, 2.639 mmol) was then added to the mixture. The mixture was allowed to sit at room temperature overnight without agitation and then transferred to an oven for aging at 40 °C for 2 days, 60 °C for 2 days, and 80 °C for 4 days. The mixture was then filtered by suction filtration, and the white solid was placed into a sealed tube and put into an oven at 100 °C for 2 days, 120 °C for 2 days, and 140 °C for 2 days. The product was collected by suction filtration and washed once with a mixture of methanol (375 mL) and diethyl ether (125 mL) and four times with 500 mL of methanol. The resulting materials were put into an oven at 150 °C for 2 days and then treated with excess trimethylsilyl chloride in ether, filtered and washed with excess ether, and finally dried again in an oven at 150 °C for 24 h.

Sodium Fulleride-Reduced Mesoporous Titanium Oxide Composite. To a suspension of a sample of trimethylsilylated mesoporous titanium oxide in dry THF was added an excess of Na_3C_{60} (synthesized by heating Na and C_{60} together in a sealed tube at 200–400 °C and characterized by XRD), as calculated on the basis of 38% Ti determined from the elemental analysis data. The mesoporous Ti solid immediately changed from a light tan color to a deep gray-black. The mixture was stirred for 1 week to ensure complete absorption of the fulleride, after which the reduced material was collected by suction filtration and washed several times with THF. Once synthesized, the material was dried in vacuo at 1×10^{-3} Torr on a Schlenk line until all condensable volatiles had been removed. This procedure was normally sufficient to remove any solvent molecules from the fulleride phase. Further reduction of this material was accomplished by addition of a predetermined quantity (calculated on the basis of the percentage of C_{60} in the material) of a stock solution of sodium naphthalene in THF to a stirred solution of the composite in THF. After the solution was stirred overnight, the material was collected by suction filtration and washed repeatedly with benzene until the washings were colorless. The material was then dried in vacuo at 1×10^{-3} Torr on a Schlenk line until all condensable volatiles had been removed. All of the materials were characterized by XRD, nitrogen adsorption and desorption, Raman spectroscopy, and elemental analysis to ensure sample quality before proceeding with the hydrogen sorption measurements.

Lithium Fulleride-Reduced Mesoporous Titanium Oxide Composite. Because of the intractable nature of lithium fullerides, the mesoporous precursors were first reduced using lithium naphthalene and then impregnated with pure C_{60}. This route was used previously by our group to synthesize mesoporous tantalum oxide−lithium fulleride composites.[49] To a benzene suspension of a sample of trimethylsilylated mesoporous titanium oxide previously reduced with 1.0 molar equiv (with respect to Ti) of lithium naphthalene was added an excess of C_{60}. After the mixture was stirred for several days to ensure complete absorption of the fullerene, the material was collected by suction filtration, washed several times with benzene, and dried in vacuo at 1×10^{-3} Torr on a Schlenk line until all condensable volatiles had been removed. All of the materials were characterized by XRD, nitrogen adsorption and desorption, Raman spectroscopy, and elemental analysis to ensure sample quality before proceeding with the hydrogen sorption measurements. This synthetic route had the advantage that materials of different Li and C_{60} ratios could readily be made by varying the quantities of these two dopants. In previous work, we found that materials treated with lower levels of Li were less effective at reducing C_{60} and therefore led to lower levels of fulleride intercalation, because the intercalation of C_{60} is a process driven by electron transfer.[47,49]

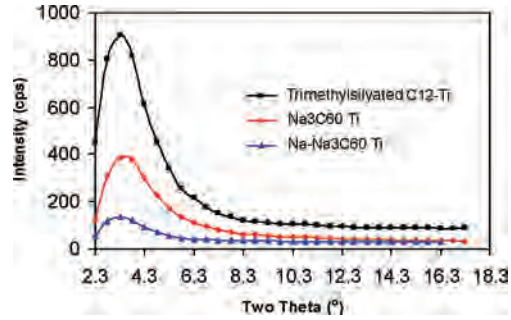

Figure 1. XRD patterns for trimethylsilylated C12-Ti, $Na_3C_{60}Ti$, and Na-$Na_3C_{60}Ti$.

Results

Sodium Fulleride-Reduced Composites. A sample of trimethylsilylated mesoporous titanium oxide having a Barret−Joyner−Halenda (BJH) pore size of 21 Å, a Brunauer-Emmet-Teller (BET) surface area of 465 m^2/g, and an XRD peak centered at $d = 30$ Å was treated with excess Na_3C_{60} in THF for 1 week until maximum absorption was achieved. This procedure yielded a new black sample that exhibited a strong XRD peak centered at $d = 30$ Å (Figure 1), which was virtually the same as that obtained from the starting material. No other peaks were found at higher angles, suggesting that there was no long-range order in the fulleride phase of the material, as observed for other 1D fulleride composites studied by our group.[44–50] The BET surface area of this new material was 116 m^2/g (Figure 2a) and the BJH pore size was 20 Å, both of which were smaller than the corresponding values for the starting material. The cumulative desorption pore volume of this sample was 0.152 cm^3/g, which also represented a decrease from the value of 0.268 cm^3/g for the starting material. These data were consistent with absorption of a large amount of the fulleride salt into the mesopores of the material. The Raman spectrum of this new composite (Figure 3a) showed an A_g band at 1462 cm^{-1}, consistent with a C_{60} oxidation state of 0.5−. It is well-known that the wavenumber of the A_g mode of pure C_{60} is 1464 cm^{-1} and that for fulleride salts of the type A_nC_{60} (A = K, Rb, Cs), this wavenumber shifts by 6 cm^{-1} for every increment in the value of n.[52] Elemental analysis (Table 1) gave values of 48.63% C and 4.57% Na, corresponding to a Na:C_{60} molar ratio of 2.94:1. In order to test the effect of further reduction on the hydrogen storage performance of this material, the parent composite was treated with 4 equiv (with respect to C_{60}) of sodium naphthalene, calculated on

(52) Kosaka, M.; Tanigaki, K.; Prassides, K.; Margadonna, S.; Lappas, A.; Brown, C.; Fitch, A. *Phys. Rev. B* **1999**, *59*, 6628.

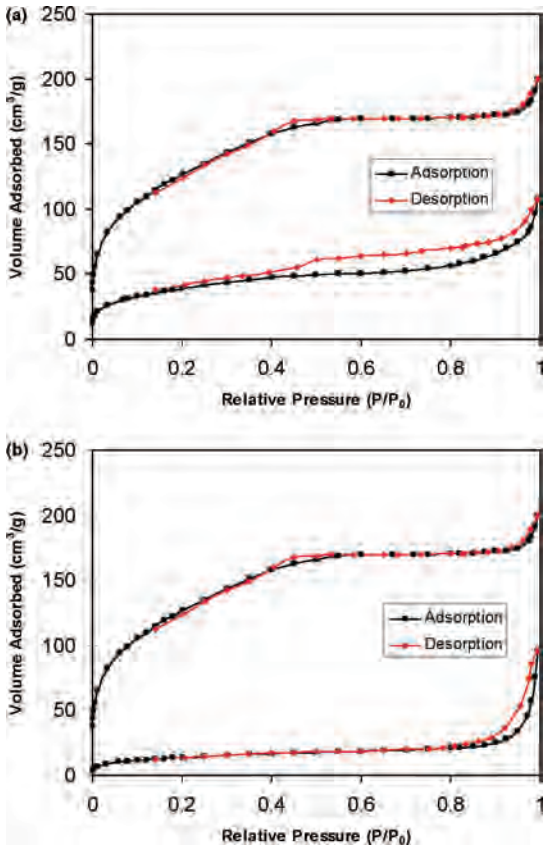

Figure 2. (a) Nitrogen adsorption/desorption isotherms of mesoporous titanium oxide (top) before and (bottom) after treatment with excess Na_3C_{60}. (b) Nitrogen adsorption/desorption isotherms of mesoporous titanium oxide (top) before and (bottom) after intercalation with excess Na_3C_{60} followed by further reduction using 4 equiv of sodium naphthalene.

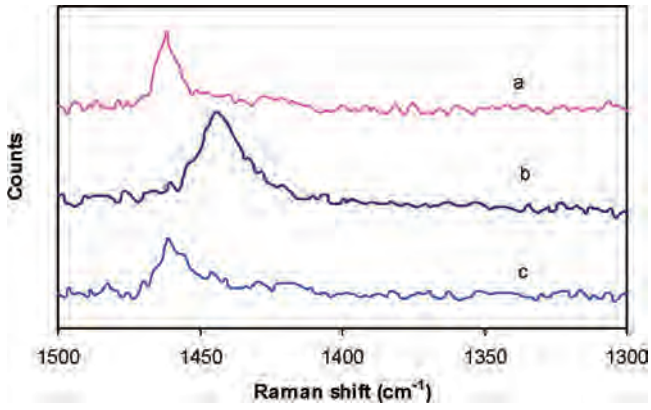

Figure 3. Raman spectra of (a) $Na_3C_{60}Ti$, (b) Na-$Na_3C_{60}Ti$, and (c) Li-$C_{60}Ti$.

Table 1. Elemental Analysis Results for Samples of Mesoporous Titanium Oxides before and after Intercalation with Alkali Metal Fullerides[a]

sample	% C	% Na	% Li	Na:C_{60} molar ratio	Li:C_{60} molar ratio
C12-Ti	3.12	NA	NA	NA	NA
$Na_3C_{60}Ti$	48.63	4.57	NA	2.94:1	NA
Na-$Na_3C_{60}Ti$	45.45	8.45	NA	6.25:1	NA
Li-C_{60}	38.78	NA	2.77	NA	8.06:1

[a] NA = not applicable.

the basis of the elemental analysis results under the assumption that all of the C in this material in excess of the residual 3.12% (see Table 1) was due to the absorbed fulleride. This

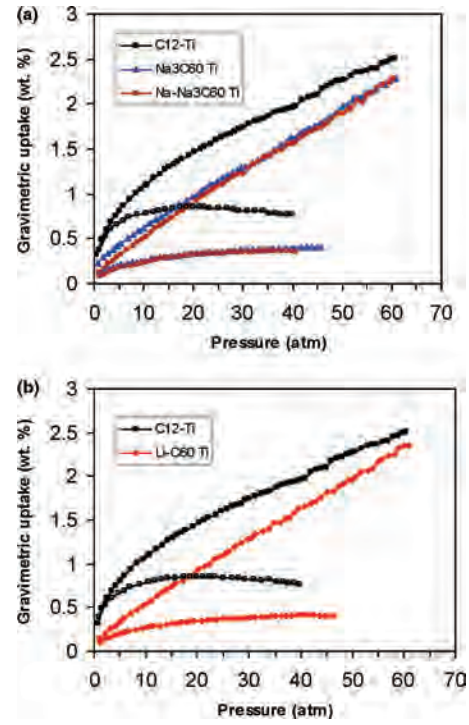

Figure 4. High-pressure gravimetric H_2 isotherms for (a) C12-Ti, $Na_3C_{60}Ti$, and Na-$Na_3C_{60}Ti$ and (b) C12-Ti and Li-$C_{60}Ti$ at 77 K. Solid symbols represent storage capacities, and open symbols denote adsorption capacities.

provided a new brown-black sample with an XRD peak centered at d = 30 Å (Figure 1), a BJH pore size of 19 Å, a BET surface area of only 50 m^2/g (Figure 2b), and a cumulative pore volume of 0.147 cm^3/g. The Raman spectrum of this new composite (Figure 3b) showed an A_g band at 1444 cm^{-1}, indicating a fulleride oxidation state of 3.5−. Elemental analysis (Table 1) gave values of 45.45% C and 8.45% Na, corresponding to a Na:C_{60} ratio of 6.25:1. The lack of substantial fulleride leaching from this material upon sodium naphthalene reduction was similar to that observed for other sodium fulleride materials studied by our group, which was attributed to the possible formation of a polymeric fulleride chain.

Hydrogen pressure−composition isotherms were recorded at 77 K for the pristine material synthesized with dodecylamine (C12-Ti), C12-Ti reduced with an excess of Na_3C_{60} ($Na_3C_{60}Ti$), and $Na_3C_{60}Ti$ further reduced with 4 equiv (with respect to C_{60}) of sodium naphthalene (Na-$Na_3C_{60}Ti$). Both H_2 storage and adsorption isotherms are displayed in Figure 4a. The adsorption (or excess storage) values reflect the amount of hydrogen bound to the surface of the porous framework, while total storage is the sum of the adsorbed H_2 and the compressed hydrogen gas in the pores. All of the hydrogen sorption results obtained in this study at 77 K and 60 atm are summarized in Table 2 along with an extrapolation of these values to 100 atm, which is a plausible pressure for onboard operating conditions. Results for Li- and Na-reduced C12-Ti materials (Li-C12-Ti and Na-C12-Ti) are also included for comparison. The storage capacities were extrapolated to 100 atm using a linear fit.

Figure 4a shows that all of the storage isotherms rose sharply at low pressure and continued to rise in a linear

Table 2. Hydrogen Sorption Capacities of Pristine C12-Ti and Corresponding Reduced Materials at 77 K

sample name	surface area (m^2/g)	apparent density (g/mL)	skeletal density (g/mL)	gravimetric adsorption (wt %)	gravimetric H_2 storage at 100 atm (wt %)[a]	volumetric adsorption (kg/m^3)	volumetric H_2 storage at 100 atm (kg/m^3)[a]
C12-Ti	531	0.724	2.678	0.85	3.51	6.154	25.48
Li-C_{60}Ti	143	0.731	2.235	0.41	3.74	2.997	27.35
Na_3C_{60}Ti	116	0.742	2.130	0.40	3.58	2.968	26.57
Na-Na_3C_{60}Ti	50	0.735	2.055	0.36	3.61	2.646	26.54
Li-C12-Ti	313	0.726	2.671	0.69	3.87	5.009	28.10
Na-C12-Ti	299	0.738	2.714	0.80	3.82	5.904	28.19

[a] Hydrogen measurement conditions were 77 K and 60 atm; results at 100 atm were obtained using a linear extrapolation having a goodness of fit (R^2) of 0.9954−0.9992.

fashion as the pressure increased from 10 to 60 atm. Reversibility was evaluated by measuring the desorption branches down to 0 atm. The desorption branches closely followed the adsorption branches without significant hysteresis. The adsorption and desorption processes were very fast, and thermodynamic equilibrium was reached within a few seconds; these results indicate that the activation barrier for these processes is very low. Unless otherwise stated, all of the hydrogen sorption capacities quoted henceforth are reversible. For the adsorption isotherms, the capacity increased with increasing pressure until saturation was reached, after which further increases in pressure led to a drop in the capacity. This feature is characteristic of excess storage isotherms,[53] which measure the amount of gas adsorbed in excess of the bulk gas that would normally occupy the dead volume of the adsorbent at that temperature and pressure. The maximum occurs when the bulk density increases at a higher rate than the adsorbed density. Extrapolation to 100 atm yielded total gravimetric and volumetric storage capacities, respectively, of 3.58 wt % and 26.57 kg/m^3 for Na_3C_{60}Ti, 3.61 wt % and 26.54 kg/m^3 for Na-Na_3C_{60}Ti, 3.51 wt % and 25.48 kg/m^3 for C12-Ti, and 3.82 wt % and 28.19 kg/m^3 for Na-C12-Ti. The gravimetric adsorption values at 60 atm were 0.40, 0.36, 0.85, and 0.80 wt % for Na_3C_{60}, Na-Na_3C_{60}, C12-Ti, and Na-C12-Ti, respectively. Intercalation with Na_3C_{60}, even when followed by further reduction using Na, clearly had little effect on the volumetric storage, while treatment involving only Na reduction provided a more substantial increase in this value. The gravimetric storage values for these materials ranged from 3.51 to 3.82 wt %, again with the material reduced only by Na displaying the highest value. The adsorption values dropped by 0.45 wt % upon intercalation of fulleride but only by 0.05 wt % upon reduction by Na only. The apparent densities of the materials all had values between 7.24 and 7.42 g/mL with no clear trend, while the skeletal densities clearly dropped by 0.5 g/mL upon fulleride inclusion, as expected on the basis of averaging the densities of amorphous titanium oxide and carbon. In our previous work,[42,43] we found that introduction of new sites and reduction of the framework of the porous structure were beneficial to hydrogen storage. On the other hand, intercalation reactions often caused losses of surface area and pore volume, which are harmful to hydrogen uptake. The observed hydrogen storage results were determined by both factors. In the present case, the reduction of the framework and concomitant inclusion of new sites on the fulleride surface could not compensate for the loss of the hydrogen uptake from the decreased surface area and pore volume, so no obvious improvement in the overall performance was observed. We had hoped that addition of fulleride would create a vast internal surface on the free fulleride sites, which would further enhance binding of hydrogen. The decreased hydrogen storage capacity for the sodium fulleride-reduced composite compared with that for the fulleride-free Na-reduced counterpart suggests the possibility that inclusion of fulleride units may have blocked access to the active Ti binding sites. This assumption can be further supported by the apparent decrease in adsorption capacity for the sodium fulleride-reduced composites compared with those for the unreduced and Na-reduced samples, since the amount of adsorption depends more strongly on the number of binding sites available in the materials than does the overall storage capacity. From Table 2, we can see that the adsorption values of 0.85 wt % and 6.154 kg/m^3 for C12-Ti and 0.80 wt % and 5.904 kg/m^3 for Na-C12-Ti were larger than the values of 0.40 wt % and 2.968 kg/m^3 for Na_3C_{60}Ti and 0.36 wt % and 2.646 kg/m^3 for Na-Na_3C_{60}Ti.

In order to replicate the initial collaborative experiments with GM, hydrogen adsorption and storage capacities of these new fulleride composites were also conducted at both room temperature and 200 °C. At elevated temperatures, adsorption in this system would likely proceed chiefly via formation of hydrides rather than by physisorption. Panels a and b of Figure 5 show gravimetric storage uptakes for all of the fulleride composites in this study at room temperature and 200 °C, respectively. The results are summarized in Table 3, along with extrapolated values at 100 atm obtained from a linear fit for comparison. At room temperature, maximum gravimetric adsorption and storage capacities, respectively, of 0.11 and 0.96 wt % were achieved for Na_3C_{60}Ti, compared with 0.10 and 0.94 wt % for C12-Ti. However, at 200 °C, both of these capacities decreased, with respective values of 0.048 and 0.62 wt % measured for Na_3C_{60}Ti, compared with 0.06 and 0.62 wt % for C12-Ti. This set of results indicates that these materials performed less efficiently at higher temperature and that reversible formation of hydrides was not favorable.

Adsorption enthalpies of both unreduced and fulleride-reduced materials were calculated from hydrogen adsorption data at 77 and 87 K, as described in the Experimental Section. The results are shown in Figure 6. The plots for Na_3C_{60}Ti and Na-Na_3C_{60}Ti show that ΔH_{ads} increased with H_2 capacity, which is consistent with our previous results

(53) Menon, P. *Chem. Rev.* **1968**, *68*, 277.

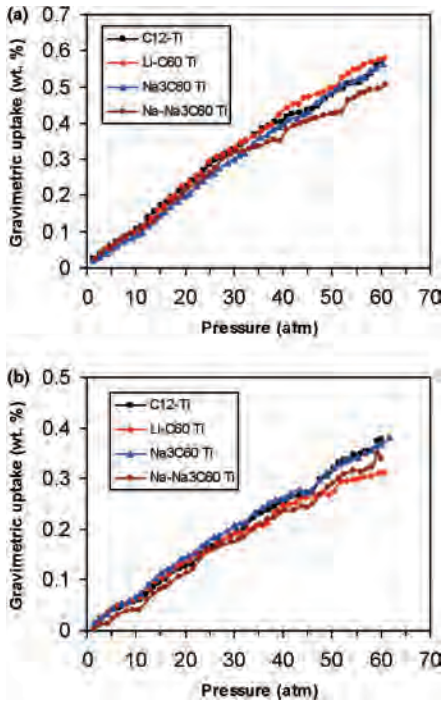

Figure 5. High-pressure H_2 gravimetric storage isotherms for the alkali fulleride-impregnated composites and unreduced material at (a) room temperature and (b) 200 °C.

Table 3. Hydrogen Sorption Capacities of Pristine and Corresponding Fulleride-Reduced C12-Ti Materials at Room Temperature (RT) and 200 °C

	gravimetric adsorption (wt %)		gravimetric storage at 100 atm (wt %)[a]	
sample	RT	200 °C	RT	200 °C
C12-Ti	0.10	0.06	0.94	0.62
Li-C_{60}Ti	0.11	0.05	0.99	0.53
Na_3C_{60}Ti	0.11	0.048	0.96	0.62
Na-Na_3C_{60}Ti	0.09	0.04	0.85	0.58

[a] Hydrogen measurements were made at 60 atm; results at 100 atm were obtained using a linear extrapolation having a goodness of fit (R^2) of 0.9868−0.9972.

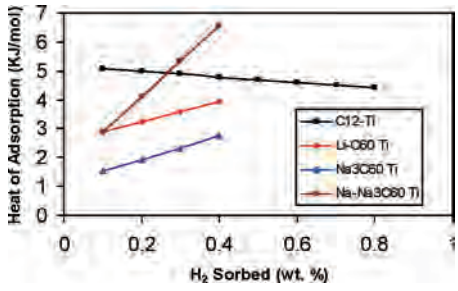

Figure 6. Enthalpies of H_2 adsorption for pristine and fulleride-reduced mesoporous titanium oxides.

involving reduced microporous titanium oxide materials.[42,43] The maximum values of ΔH_{ads} for Na_3C_{60}Ti and Na-Na_3C_{60}Ti were 2.74 and 6.55 kJ/mol, respectively, compared with 5.42 kJ/mol for Na-C12-Ti. This follows the trend of increasing reduction of the Ti oxide framework, demonstrating once again the positive effect of reduction on binding enthalpies in this system.

Li-Fulleride-Reduced Composites. In order to gauge the effect of alkali cation size on this system, the analogous lithium fulleride composite was prepared. When trimethylsilylated C12-Ti was treated with lithium naphthalene followed by C_{60}, the new black material that was formed had an XRD pattern virtually identical to that of trimethylsilylated C12-Ti (Figure 7), a BET surface area of 143 m^2/g, a BJH pore size of 20 Å, and a pore volume of 0.156 cm^3/g. The nitrogen adsorption/desorption isotherms of this material are shown in Figure 8. These data are consistent with retention of the mesostructure and partial filling of the channels with fulleride units. The Raman spectrum of this new material (Figure 3c) exhibited an A_g band at 1461 cm^{-1}, corresponding to a C_{60} oxidation state of 0.5−. Elemental analysis of this material gave 38.78% C and 1.15% H, compared with 3.12% C and 1.36% H in the mesoporous titanium oxide starting material. The percentages of Li and Ti in the composite material were 2.77 and 26.3%, respectively, giving a Li:Ti:C molar ratio of 0.72:1:5.88. The corresponding Li:C_{60} ratio was 8.06:1.

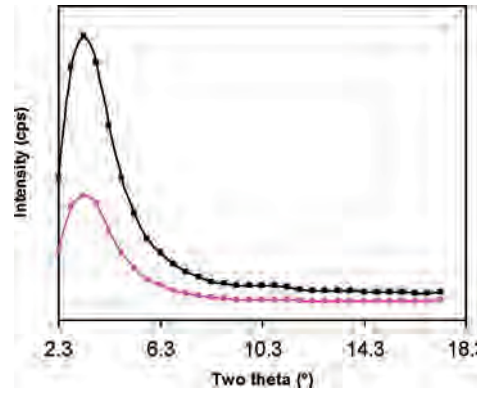

Figure 7. XRD patterns of mesoporous titanium oxide (top) before and (bottom) after treatment with 1 equiv of lithium naphthalene followed by doping with excess C_{60}.

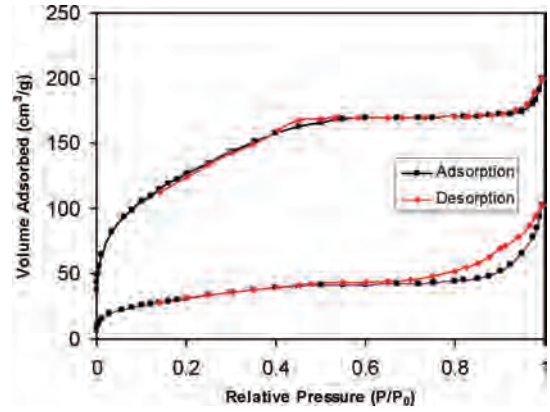

Figure 8. Nitrogen adsorption/desorption isotherms of (top) C12-Ti and (bottom) Li-C_{60}Ti.

Hydrogen pressure−composition isotherms at 77 K for both adsorption and storage for C12-Ti reduced with 1 equiv of lithium naphthalene and then doped with the maximum amount of C_{60} (Li-C_{60}Ti) are shown in Figure 4b. This material yielded total storages of 3.74 wt % and 27.35 kg/m^3 in gravimetric and volumetric uptake, respectively, at 100 atm. The greater surface area and pore volume of this sample compared with those of Na_3C_{60}Ti and Na-Na_3C_{60}Ti may have been responsible for the small increases in the gravimetric and volumetric densities observed for Li-C_{60}Ti. The hydrogen

adsorption capacities of Li-C_{60}Ti, which had values of only 0.41 wt % and 2.997 kg/m^3, were smaller than those of the pristine and Li-reduced samples; this result can be explained by the decreases in surface area and pore volume, the smaller degree of surface reduction, and the decrease in the number of hydrogen binding sites resulting from blockage by the intercalated fulleride units. Table 3 shows that the gravimetric adsorption and storage capacities, respectively, for this sample were 0.11 and 0.99 wt % at room temperature and 0.05 and 0.53 wt % at 200 °C, similar to those of the Na analogues. The hydrogen adsorption enthalpy of this material is illustrated in Figure 6. As with Na_3C_{60}Ti and Na-Na_3C_{60}Ti, the enthalpy increased with the H_2 capacity. The maximum ΔH_{ads} for Li-C_{60}Ti was 3.94 kJ/mol, compared with 5.44 kJ/mol for Li-C12-Ti.

Discussion

The volumetric storage capacities of this series of fulleride composites are not obviously improved compared with those of the pristine samples by the inclusion of fulleride units in the pores. This outcome may be attributed to several factors. First, alkali fullerides are much weaker reducing agents than alkali metals or organometallic compounds of transition metals, as demonstrated by our previously reported results obtained using XPS binding energies.[44–50] The mean oxidation state of Ti in mesoporous titanium oxide reduced by excess K_3C_{60} was 3.7+.[46] Since our previous work showed that hydrogen binding to transition metals strongly depends on the electron density at the metal, the sodium fulleride-reduced Ti material should have had a weaker interaction with hydrogen than its sodium-reduced counterpart, which had Ti in the 3+ oxidation state. Also, the impregnated fulleride units may block access to active, coordinately unsaturated Ti metal centers, since fulleride addition dramatically decreased the hydrogen adsorption capacity of the materials compared with those of the pristine and fulleride-free alkali metal-reduced materials, even when the skeletal densities of the fulleride-reduced composites were less than those of the pristine and alkali metal-reduced samples. In previous electrochemical studies comparing charge transfer inside the pores of Li-reduced mesoporous tantalum oxide with that in the same material impregnated with C_{60}, the C_{60} units hindered rather than facilitated electron transfer through the pores.[49] This result was surprising given the well-known conductive properties of fullerides and was attributed to steric hindrance of the Li counterions by the fullerides. Thus, steric blockage effects may also play a role in the hydrogen storage properties of this system. The fulleride units not only reduced the pore volume of the material, thus decreasing the amount of compressed gas residing in the pores, but may also have disrupted binding to the titanium oxide surface through steric contact. While these effects might have been expected, the major disappointment of this study is that binding of hydrogen to the surface of the fulleride units did not compensate for these losses, as expected on the basis of the high sorption capacities of many carbon-based materials.

The increases in adsorption enthalpies with increasing hydrogen uptake amount were consistent with our previously reported results.[42,43] However, the enthalpies of the alkali fulleride-impregnated materials were less than those of their fulleride-free Na- and Li-reduced counterparts. In the lithium fulleride composites, this can be explained by the transfer of electron density from the walls to the electronegative fullerene phase. This process diminishes the electron density of the Ti in the mesoporous surface. For the sodium fulleride composite, the decreased amount of framework reduction compared with that of Na-C12-Ti can explain the decreased hydrogen adsorption enthalpy for this material. The increased enthalpy of Na-Na_3C_{60}Ti compared with that of Na-C12-Ti can be explained by the higher level of reduction resulting from treatment with sodium naphthalene. Since all other carbon-based physisorption materials show decreasing enthalpies with increasing coverage, the reduced titanium oxide surface must provide the majority of the binding sites in these composites.

Conclusion

In this study, titanium oxide−alkali fulleride composite materials were synthesized and characterized by nitrogen adsorption, XRD, Raman spectroscopy, and elemental analysis. The adsorption capacities of these new composites at 77 K were smaller than those of the unreduced pristine sample and materials reduced only with Na or Li, while the overall storage capacity barely increased. This was attributed to the decreased amount of reduction of the titanium oxide framework, blockage of active binding Ti sites by the intercalated fulleride units, and loss of surface area and pore volume without sufficient compensation by the fulleride surface. The hydrogen sorption of these new composites at room temperature and 200 °C showed even more disappointing results. The results from this work and our previous studies show that a highly reduced framework combined with accessible unsaturated metal centers, high surface area, and large pore volume are needed to achieve useful hydrogen storage capacity.

Acknowledgment. The authors wish to acknowledge the Natural Science and Engineering Research Council of Canada for funding.

IC701762E